BOLETIN DE LA SOCIEDAD ESPAÑOLA DE
Cerámica y Vidrio
A R T I C U L O

Studies on Perovskite-Based Electrodes for Symmetrical SOFCs

A.J. DOS SANTOS-GARCÍA [1], J.C. RUIZ-MORALES [2] and J. CANALES-VÁZQUEZ [1]

[1] Instituto de Energías Renovables, Universidad de Castilla la Mancha-Parque Científico y Tecnológico de Albacete, 02006 Albacete, Spain.
[2] Departamento de Química Inorgánica, Universidad de La Laguna, 38200 La Laguna, Spain.

The use of the same material as anode and cathode in symmetrical solid oxide fuel cells (SFCs) promises notable benefits as easier fabrication, hence lower cost production and resistance to carbon formation upon fuel cracking. Although chromites and chromo-manganites have been proposed as candidate electrode materials for this novel SOFC configuration, demonstrating promising performances, further work is required to develop compositions exhibiting higher efficiencies. In the present work we evaluate the structural evolution from cubic to orthorhombic unit cells with increasing the Fe content and the performance of $La_4Sr_8Ti_{12-x}Fe_xO_{38-\delta}$ (LSTF) phases and compare their response with other symmetrical electrodes. The electrochemical performance is 20% higher when using graded LSTF electrodes than in other perovskite-based systems.

Keywords: Solid Oxide Fuel Cells, Symmetrical solid oxide fuel cells, electrodes, perovskite, composites.

Electrodos basados en Perovskita para pilas de combustible SOFC simétricas

La utilización simultánea de un mismo material cerámico como ánodo y cátodo en pilas de combustible de óxido sólido simétricas (SFCs) aporta una serie de beneficios entre los que figura una fabricación más sencilla, reducción de los costes de producción, así como resistencia a la formación de depósitos de carbón por craqueo del combustible. Recientemente, cromitas y cromomanganitas han sido propuestos como materiales capaces de adoptar esta novedosa configuración SOFC y, si bien los resultados obtenidos son prometedores, se requiere de una mayor investigación para el desarrollo de nuevas composiciones que presenten eficiencias más elevadas. En el presente trabajo, se evalúan la evolución de la estructura desde celdas cúbicas a ortorrómbicas al aumentar el contenido en Fe y las prestaciones del sistema $La_4Sr_8Ti_{12-x}Fe_xO_{38-\delta}$ (LSTF) y se compara su respuesta con otros electrodos simétricos, observándose que el rendimiento es hasta un 20% mayor en el caso de emplear electrodos LSTF que en otros sistemas basados en perovskitas.

Palabras clave: Pilas de Combustible de Óxido Sólido, Pilas de combustible de óxido sólido simétricas, electrodos, perovskitas, composites.

1. INTRODUCTION

Fuel cells are at the forefront of the emerging clean technologies that promise efficient power generation to substitute traditional methods based on the combustion of fossil fuels. Among them, solid oxide fuel cells promise high efficiencies and tolerance to fuels as a consequence of their relatively high operating temperatures (600-1000ºC) required for adequate levels of oxide ion mobility in the solid electrolyte. ZrO_2 substituted with 3-12% of Y_2O_3 (YSZ) is the most commonly used electrolyte material, whereas a ceramic-metal composite Ni-YSZ is usually chosen as anode and Sr-substituted $LaMnO_3$ as cathode. Over the last decade, several strategies have been adopted in the search for efficient devices that may operate under hydrocarbon feed in the intermediate temperature range (below 800ºC), some of them related to the development of novel anode materials for direct hydrocarbon operation and/or the use of ceria-based or perovskite-based electrolytes. Indeed, some of the alternatives to Ni-YSZ cermets such as Cu-based cermets and perovskite-based phases (1-4) exhibit rather competitive performances, especially the former materials.

Nevertheless further progress may also be achieved via the use of well-known materials considering approaches such as the optimisation of the microstructure using various routes, i.e. pore formers, infiltration techniques, organic templates, etc (1,5-6). In this context, a novel concept of SOFC has been recently proposed: the symmetrical fuel cell (SFC), which consists of the use of the same material as anode and cathode. The reduction in the number of different cell components would imply certain benefits related to easier fabrication processes and management. It should be noted that coke formation could be avoided by reversing the gas flows, i.e. periodically the starting anode becomes the cathode and receives oxygen that would remove any carbonaceous deposit formed on the electrode surface. Although the requirements of the candidate materials are rather restrictive, Irvine and co-workers (7) and several other research groups (8-9) have

proved the validity of this concept in the high temperature range. The first reports were focused on lanthanum-strontium chromo-manganites (LSCM) based composites, exhibiting power densities of approximately 0.5 and 0.3 Wcm^{-2} under humidified H_2 and CH_4 atmospheres respectively at 950 °C (8). Chromites commonly used as interconnects have also been evaluated in symmetric configuration, although the performances were more modest (10), possibly due to the poor catalytic activity of these phases towards fuel oxidation (11).

Perovskite-based titanates have been usually considered as potential anode materials or anode support (current collector) as they exhibit high conductivity, stability under reducing conditions, S-tolerance and do not react with the state of the art electrolytes (12-15). On the other hand, ferrites substituted with Ti in the B-site have been extensively studied as mixed conducting oxide membranes and/or SOFC cathode materials (16-18) due to their high mixed (ionic-electronic) conductivity and chemical compatibility with YSZ electrolytes. In a previous work, the Ti-rich part of the $La_4Sr_8Ti_{12-x}Fe_xO_{38-\delta}$ solid solution was explored in the search for symmetric electrode materials (19). Although the performances were rather modest, the relatively high OCVs when operating under methane suggested that these phases could find application in SFCs upon further optimisation. Herein, we present some further information regarding phases with $0.0 \leq x \leq 6.0$ and compare them with other symmetrical electrode candidate materials.

2. EXPERIMENTAL SECTION

$La_4Sr_8Ti_{12-x}Fe_xO_{38-\delta}$ (LSTF), $La_{0.75}Sr_{0.25}Cr_{0.5}Mn_{0.5}O_{3-\delta}$ (LSCM) and $La_{0.7}Ca_{0.3}CrO_{3-\delta}$ (LCC) phases were prepared via the traditional solid state reaction. Pre-dried stoichiometric amounts of the corresponding oxides and carbonates (>99%, Aldrich) were milled in zircona ballmills using acetone as solvent for 30 minutes and then fired at 1100-1200°C for 6-12 hours. The resulting powders were milled again for 30 minutes and pressed uniaxially into pellets at 1 metric ton. The pellets were then fired at 1300-1500 °C for 48 hours, showing relative densities >90% after sintering.

The structure of LSTF was investigated by combining X-ray diffraction (XRD) and transmission electron microscopy (TEM). XRD experiments were performed on a PANalytical diffractometer equipped with a X'Celerator detector with monochromatic $CuK_{\alpha 1}$ radiation ($\lambda = 1.54056$ Å) in the 2θ range 10º-110º, scan step size of 0.01 for 1.5s. Rietveld refinements of the data were performed using the Fullprof program (20). The backgrounds were fitted using a linear interpolation and peak shapes were modelled by a Thompson Cox Hasting function. Compatibility studies of the electrode materials with the YSZ electrolytes used in the present study were carried out by firing an intimate mixture of 1:1 YSZ:LSTF powders up to 1350°C in air for several hours.

TEM studies were carried out on a Jeol 2011 electron microscope operating at 200 kV and equipped with a ±20° double-tilt sample holder and an Oxford Link EDS detector. Samples were prepared by dispersing finely ground ceramic powder in acetone and depositing a drop of the resulting dispersion on a perforated C-coated Cu grid.

Polarisation studies were performed using 2 mm thick fully-dense YSZ electrolytes prepared as described elsewhere [8,19] coated with 1:1 LSTF:YSZ, LSCM:YSZ and LCC:YSZ electrodes and a thin layer of Pt on top under $3\%H_2O/4\%H_2/93\%Ar$, $3\%H_2O/97\%H_2$ and $3\%H_2O/97\%CH_4$. These studies were carried out on a 1260 Solartron frequency response analyser in the 0.1 Hz-1 MHz range applying a 50 mV signal.

LSTF, LCC and LSCM electrodes for fuel cell testing were prepared by applying a thin layer (typically 50μm) of 1:1 LSTF:YSZ composites mixed with binder (Decoflux WB41, Zschimmer and Schwartz) on both sides of the YSZ electrolyte and fired at 1200 °C for 2 hours to ensure good adherence. In the case of LSTF electrodes a fine layer of Au and Pt was used at the anode and the cathode respectively to act as a current collector to avoid any possible catalytic activity, as Pt favours the electrochemical oxidation of methane. It could be argued that Pt also favours oxygen reduction, though the effect on a high-temperature fuel cell is less marked and Pt is commonly used as current collector at the cathode in laboratory tests [1]. Pt was also used as current collector in LSCM and LCC-based electrodes.

The fuel cell tests were performed on a two electrode setup (8,19) using humidified 5% H_2/Ar, H_2 and CH_4 as fuels and O_2 as oxidant at the cathode (flow rates 150-200 ml/min). The polarisation measurements were carried out using a IM6e Zahner unit at open circuit voltage conditions in the $0.1\text{-}3x10^5$ Hz frequency range using a 50 mV perturbation in the 950-800°C temperature range. Cyclic-voltammetries at $4\text{-}12mVs^{-1}$ were also performed using the same equipment.

The microstructure of the cells measured (top view and cross sections) was monitored by SEM on a JSM-6300 Jeol electron microscope operating at 5-30 kV.

3. RESULTS AND DISCUSSION

3.1. Structural characterisation.

The n=12 member ($La_4Sr_8Ti_{12}O_{38-\delta}$) of the $La_4Sr_{n-4}Ti_nO_{3n+2}$ series has been previously described as a XRD cubic phase (13,21). The introduction of Fe in the B-sites does not result in the formation of $La_2Ti_2O_7$-like layered domains in the crystals as can be observed in figure 1. This is a critical parameter as the formation of layers causes a dramatic decrease of the electronic conductivity, preventing potential applications as fuel cell electrodes (3). On the other hand, oxygen-vacancy ordering has been extensively described in perovskite-based ferrites (22), giving rise to intermediate structures between the primitive perovskite and brownmillerite as a result of ordered layers along the b-axis. In the present case, there was no evidence of long-range ordering along a particular crystallographic direction, although there are regions where an incipient microdomain texture is evident (figure 1b). Consequently, the presence of Grenier-like phases (22 and references therein) has not been considered during refinement.

The substitution of Ti by Fe in the perovskite B-sites causes a gradual distortion of the cubic perovskite unit cell, s.g. Pm-3m (x=0), i.e. diffraction maxima split as the Fe content increases and some weak superlattice peaks also appear due to reverse octahedra tilting in consecutive layers. Although the peak splitting of the originally cubic reflections is subtle, structural transitions from Pm-3m to I4/mcm to Imma and finally to Pnma with increasing x in the $La_4Sr_8Ti_{12-x}Fe_xO_{38-x}$ solid solution occur. It is worth noting that not all the superlattice reflections can be detected by XRD as they depend on weak anion scattering.

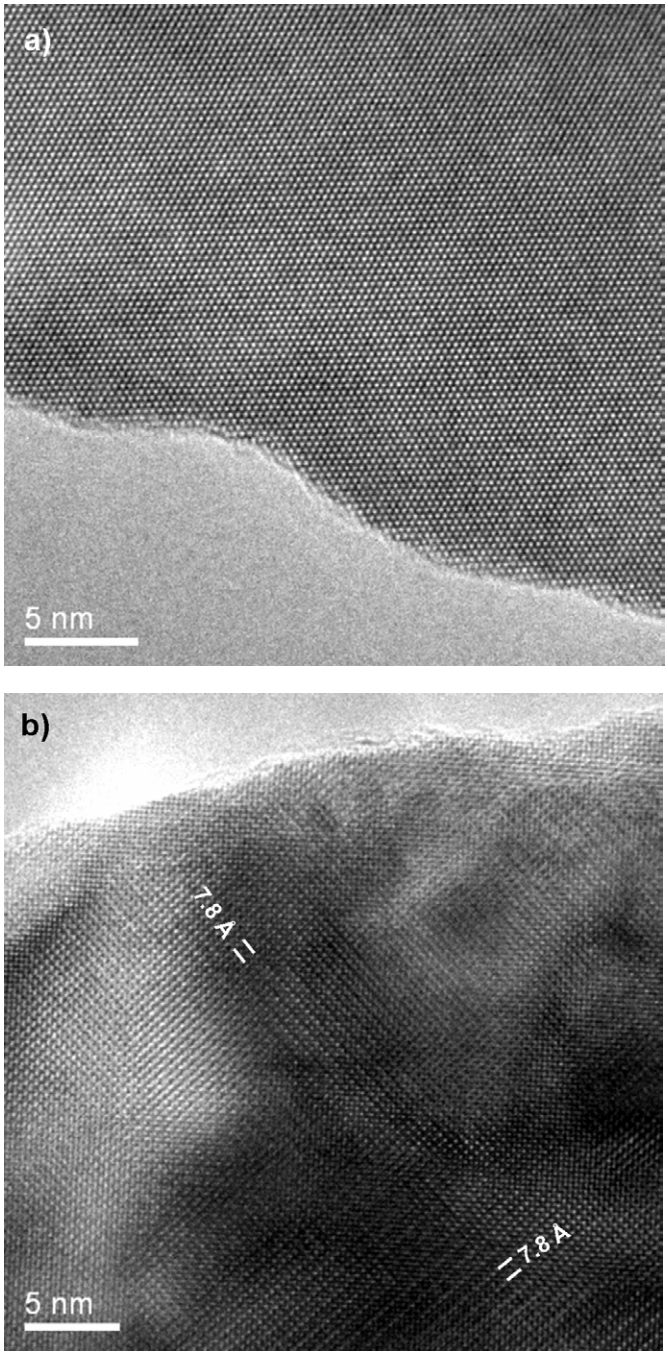

Fig. 1- TEM micrographs corresponding to a view down the $[111]_c$ (a) and the $[110]_c$ for $La_4Sr_8Ti_7Fe_5O_{38-x}$. No $La_2Ti_2O_7$-like layers were observed (a), although some crystals exhibited microstructure texture (b) common in tetragonal and orthorhombic perovskites.

x>0.5 x>1.5 x>3.0

Cubic → Tetragonal → Pseudo-tetragonal → Orthorhombic

Pm-3m I4/mcm Imma Pnma

The first structural cell distortion observed in the $La_4Sr_8Ti_{12-x}Fe_xO_{38-x}$ system, a Pm-3m to I4/mcm transition for x>0.5, involves a continuous change. For x>1.5, a second structural transition is observed, i.e. the symmetry changes from I4/mcm to Imma in a first order transition, which is discontinuous as the structure changes from having tilts around the tetrad axis ($a^0a^0c^-$) to tilts around a diad axis of the oxygen octahedra ($a^0b^-b^-$). At higher Fe contents (x>3.0), there is a Imma to Pnma transition, without symmetry discontinuity as involves gain/loss of the in-phase tilting. This phase transition sequence is rather habitual in perovskites with both increasing x in the solid solution (23) and/or temperature (24) and similar results have been reported for related ferrite-titanate systems (16-17). Figure 2 shows a segment from the observed and calculated diffraction patterns for Fe contents x=0, 0.5, 2.5 and 3.0. In figure 2a neither distortions nor superlattice reflections are apparent in the non-substituted phase in agreement with previous reports (21). However and as mentioned above, the introduction of Fe results in the presence of superlattice reflections due to octahedra tilting (marked with an arrow) and splitting of the main cubic reflections (figures 2b-c). It is interesting to note that there is a reversal of the intensities in the 200 cubic reflection pair (figures 2b-c), which implies a transition from I4/mcm to the Imma pseudo-tetragonal space group (25). Figure 2d shows the pseudo-orthorhombic distortion from the 200 cubic reflection that splits to the combination of the 220 and 004 reflections corresponding to the Pnma space group.

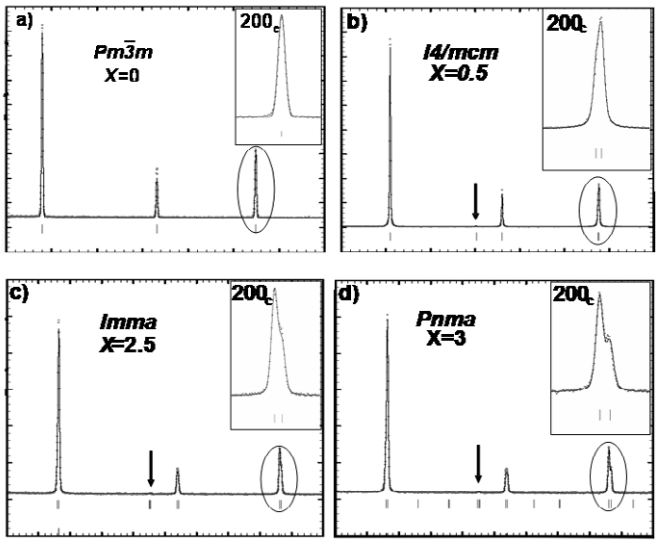

Fig. 2- Segments from the observed diffraction patterns from LSTF with x=0, 0.5, 2.5 and 3.0. The continuous line corresponds to the calculated by the Rietveld method assuming the Pm-3m (a), I4/mcm (b), pseudo-tetragonal Imma (c) and pseudo-orthorhombic Pnma (d) space groups respectively.

Regarding XRD pattern refinement, the perovskite A-sites were fully occupied at random by 2 Sr and 1 La, whilst Ti and Fe were placed in the B sites. In this structural model, such a situation was treated by assigning to the different atoms the same x,y,z site and the same displacement parameters U_{ij}. As there was a strong correlation between the site occupancy and the displacement factor, it was preferable to refine them in alternating cycles until convergence. Assuming that there existed a certain number of oxygen vacancies, the corresponding oxygen site occupancy was varied freely until the final value was reached (26). Table 1 gives the refined cell parameters as well as the fit agreement factors obtained for several compositions.

TABLE. REFINED CELL PARAMETERS AND THE FIT AGREEMENT FACTORS OBTAINED USING RIETVELD REFINEMENT CORRESPONDING TO THE $La_4Sr_8Ti_{12-x}Fe_xO_{38-\Delta}$ SERIES FOR COMPOSITIONS 0≤X≤5.5.

	x=0.0	x=0.5	x=1.0	x=1.5	x=2.0	x=2.5	x=3.0	x=5.5
S.G.	Pm-3m	I4/mcm	I4/mcm	Imma	Imma	Imma	Pnma	Pnma
a (Å)	3.9061(1)	5.5384(1)	5.5376(1)	5.5439(1)	5.5406(1)	5.5553(1)	5.5617(1)	5.5413(1)
b (Å)	3.9061(1)	5.5384(1)	5.5376(1)	7.8190(1)	7.8194(1)	7.8267(1)	7.8278(1)	7.8085(1)
c (Å)	3.9061(1)	7.8433(1)	7.8424(1)	5.5323(1)	5.5321(1)	5.5389(1)	5.5415(1)	5.5233(1)
V(Å^3)	59.599(2)	240.582 (5)	240.486(5)	239.816(5)	239.676(6)	240.827(6)	241.250(4)	238.988(6)
R_p	7.92	7.94	7.57	6.86	8	4.99	4.25	6.84
R_{wp}	10.6	9.93	9.39	8.77	10.7	6.92	5.46	8.79
R_{Bragg}	4.54	3.23	3.65	3.84	6.06	4.09	5.28	6.16
χ^2	1.3	3.37	2.96	2.5	2.77	1.71	1.22	1.97

The compatibility studies performed after firing intimate mixtures of LSTF powders with YSZ and CeO_2 revealed that no significant chemical interaction occurs as the diffraction peaks remain nearly unchanged up to fabrication temperature (figure 3), which is consistent with previous reports on similar compositions and other titanate-based electrodes (16-17).

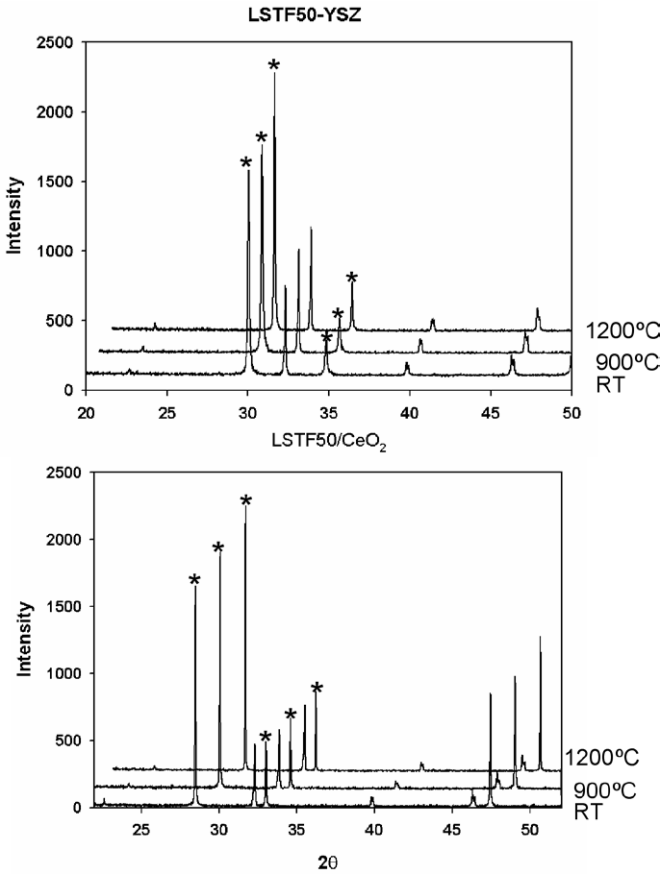

Fig. 3- XRD patterns corresponding to intimate mixtures of LSTF:YSZ (a) and LSTF:CeO_2 (b) fired at different temperatures. No chemical interaction was observed after the annealing process. The asterisks (*) denote YSZ and CeO_2 diffraction peaks respectively.

3.2. Electrochemical characterisation

It has been previously reported that the overall conductivity of the $La_4Sr_8Ti_{12-x}Fe_xO_{38-x}$ ($0<x<6.0$) system increases with increasing the Fe content under both oxidising and reducing conditions (19). The electrocatalytic properties followed a similar trend and therefore the Fe-rich compositions (x=5.0, 5.5 and 6.0) were considered as the most adequate electrode candidates for symmetric fuel cells. Figure 4 corresponds to the polarisation resistance of the x=5.0 composition compared with LSCM and LCC-based electrodes in air and 5%H_2/Ar. In all cases the responses in oxidising conditions are much lower, which implies that the systems studied (including Pt and Au pastes) are more electrocatalytically active towards oxygen reduction than hydrogen oxidation, i.e. they perform better as cathodes rather than anodes. Arguably the presence of Pt at the cathode may play an important role in the responses observed, although Pt itself is considered as a poor

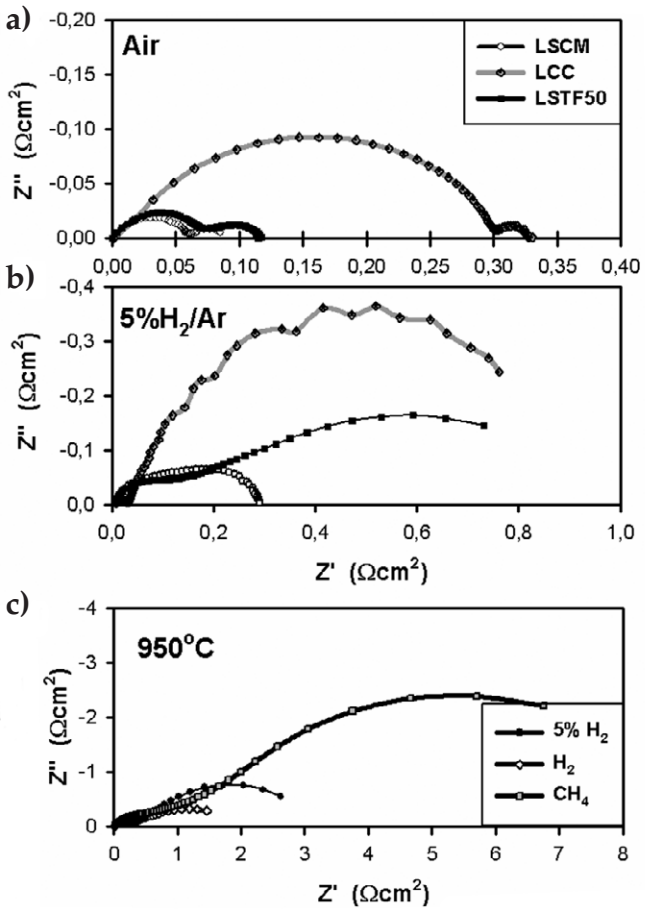

Fig. 4- Impedance plots showing the polarisation resistances corresponding to LSTF, LCC and LSCM:YSZ electrodes measured under air (a) and 5%H_2/Ar (b). (c) Impedance plots corresponding to the overall cell impedance of SFCs using $La_4Sr_8Ti_7Fe_5O_{38-x}$-based electrodes in 5%H_2/Ar, H_2 and CH_4 at 950ºC.

SOFC cathode. The responses of LSTF were better than those reported in (19) possibly due to differences in the microstructure. Obviously, these polarisation values are rather high compared to the state of the art SOFC electrode materials (typically 0.1 Ωcm^2), though further optimisation via the use of graded compositions, optimisation of the microstructure or the addition of phases with catalytic activity may reduce the gap.

Regarding cell performance, at 950°C the overall cell polarisation values are 3.4, 2.4 and 9.8 Ωcm^2 under $3\%H_2O/4\%H_2/93\%Ar$, $3\%H_2O/97\%H_2$ and $3\%H_2O/97\%CH_4$ respectively (figure 4c). It is very important to note that contrary to the previous results, the values in the present work have been obtained using Au as current collector at the anode rather than Pt. The use of Pt as current collector at the anode is rather controversial as this noble metal exhibits catalytic properties towards hydrocarbon oxidation, hence potentially masking the real response coming from the ceramic material. Although, Au nanoparticles are also well-known for their catalytic activity in redox processes (27), the temperature range considered in the present work is very close to the melting point, which implies that Au agglomerates and thereby acts mostly as current collector. Moreover, metal coarsening may have a negative impact as large Au clusters can certainly block the electrode pores, hence preventing the access of gases to the active sites.

Nevertheless, it should be pointed out that LSTF-based electrodes render power and current densities under pure hydrogen similar to those LSCM and LCC-based electrodes, i.e. 100 $mWcm^{-2}$ at 950ºC (figure 5). The performance under methane is rather modest in terms of maximum power densities, although it is important to note that an optimisation of the electrode composition, i.e. use of graded compositions and the use of CeO_2 to enhance the catalytic properties, may result in enhanced open circuit voltages (OCVs). For instance, the use of a two layered electrode, i.e. 1:1 LSTF:CeO_2 layer on top of a 1:1 LSTF:YSZ layer, renders OCVs in excess of 1 V, which is 15-20% more than the results reported for other perovskite-based SFC electrodes, including simple LSTF electrodes. In other words, an adequate optimisation of LSTF-based electrodes could yield in theory higher current and power densities. Although further research work is required to determine exactly such enhanced voltage values, it is likely that these electrodes present certain activity towards methane oxidation.

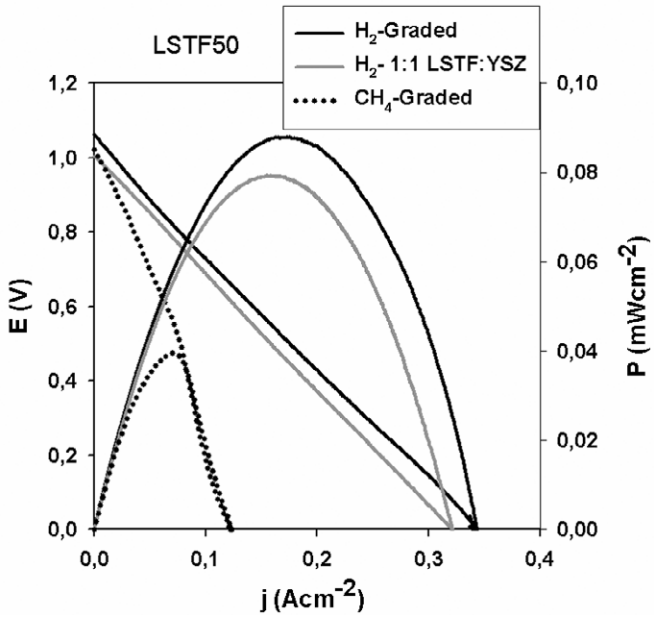

Fig. 5- j-E plots corresponding to standard 1:1 LSTF:YSZ and a graded electrode operating at 950ºC. Under methane, relatively high OCV values are obtained (>1.0V).

4. CONCLUSIONS

In the present work, $La_4Sr_8Ti_{12-x}Fe_xO_{38-\delta}$ phases have been investigated for their potential application as electrodes for high temperature symmetric fuel cells. The structural characterisation revealed that the introduction of Fe in the n=12 member of the $La_4Sr_{n-4}Ti_nO_{3n+2}$ series does not give rise to the formation of $La_2Ti_2O_7$-like oxygen-rich layers that usually result in drastic drops of the electronic conductivity. However the introduction of Fe in the perovskite B-sites causes a distortion of the parent XRD cubic unit cell through to orthorhombic symmetries. This is accompanied by a gradual increase of the overall conductivity and also in the electrochemical activity of these materials for both oxygen reduction and hydrogen oxidation as previously observed (19).

Compared with other symmetric electrode candidate materials recently reported in the literature, Fe-substituted LST based-electrodes offer rather promising performances in fuel cells fed with hydrogen, although further research work is highly demanded to optimise both the microstructure and graded compositions. Indeed, preliminary results on two-layered electrodes, i.e. a 1:1 LSTF:YSZ plus a 1:1 LSTF:CeO_2 exhibit enhanced performances compared to the simpler 1:1 LSTF:YSZ electrodes and other perovskite-based composites (LSCM or LCC). This is especially relevant when using methane as fuel, as the use of graded electrodes results in OCVs in excess of 1.0 V, i.e. 15-20% larger than in the case of habitual symmetric electrodes, including LSTF simpler electrodes, which in theory implies higher power and current densities.

ACKNOWLEDGEMENTS

The authors are indebted to the Albacete Science and Technology Park, Universidad de Castilla la Mancha and the Ramón y Cajal Program (MEC) for financial support. The Serveis de Microscòpia at UAB (Bellaterra) are also acknowledged for providing access to the electron microscopes.

REFERENCES

1. a) S. Park, J. M. Vohs and R. J. Gorte, « Direct Hydrocarbon oxidation in a solid oxide fuel cell», Nature, 404, 265-268 (2000); b) R. Craciun, S. Park, R.J. Gorte, J.M. Vohs, C. Wang and W.L. Worrell, J. Electrochem. Soc., «A novel method for preparing anode cermets for solid oxide fuel cells», 144, 4019-4022 (1999); c) C. Lu, W.L. Worrell, R.J. Gorte and J.M. Vohs, «SOFCs for Direct Oxidation of Hydrocarbon Fuels with Samaria-doped Ceria Electrolyte», J. Electrochem. Soc., 150(3), A354 (2003).
2. a) S. Tao and J. T. S. Irvine, «A redox-stable efficient anode for solid-oxide fuel cells", Nat. Mater., 2, 320 (2003); b) S. Tao and J. T. S. Irvine, «Synthesis and Characterization of $(La_{0.75}Sr_{0.25})Cr_{0.5}Mn_{0.5}O_{3-\delta}$, a Redox-Stable, Efficient Perovskite Anode for SOFCs», J. Electrochem. Soc., 151, A252-A259 (2004).
3. a) J. C. Ruiz-Morales, J. Canales-Vázquez, C. Savaniu, D. Marrero-López, W. Zhou and J. T. S. Irvine, «Disruption of extended defects in solid oxide fuel cell anodes for methane oxidation», Nature, 439, 568-571 (2006); b) J. C. Ruiz-

Morales, J. Canales-Vázquez, D. Marrero-López, C. D. Savaniu, P. Núñez, W. Zhou and J. T. S. Irvine, Phys. Chem. Chem. Phys., 9, 1821 (2007).
4. a) Y.H Huang, R.I. Dass, Z.L. Xing and J.B. Goodenough, «Double Perovskites as Anode Materials for Solid Oxide Fuel Cells», Science, 312 (5771), 254-257 (2006) 254; b) Y.H. Huang, R.I. Dass, J.C. Denyszyn and J.B. Goodenough, «Synthesis and characterization of $Sr_2MgMoO_{6-\delta}$-An anode material for solid oxide fuel cell», J. Electrochem. Soc., 153(7), A1266 (2006).
5. M.D. Gross, J.M. Vohs and R.J. Gorte, «Recent progress in SOFC anodes for direct utilization of hydrocarbons», J. Mater. Chem, 17, 3071-3077 (2007).
6. J. C. Ruiz-Morales, J. Canales-Vázquez, J. Peña-Martínez, D. Marrero-López, J. T. S. Irvine and P. Núñez, «Microstructural optimisation of materials for SOFC applications using PMMA microspheres», J. Mater. Chem., 16, 540-542 (2006).
7. D.N. Bastidas, S.Tao and J.T.S. Irvine, «A symmetric solid oxide fuel cell demonstrating redox stable perovskite electrodes», J. Mater. Chem., 1603-1605 (2006).
8. J. C. Ruiz-Morales, J. Canales-Vázquez, J. Peña-Martínez, D. Marrero-López and P. Núñez, «On the simultaneous use of $La_{0.75}Sr_{0.25}Cr_{0.5}Mn_{0.5}O_{3-\delta}$ as both anode and cathode material with improved microstructure in Solid Oxide Fuel Cells», Electrochim. Acta 52 [1], 278-284 (2006).
9. a) S.P. Jiang, L.Zhang and Y. Zhang, «Lanthanum strontium manganese chromite cathode and anode synthesized by gel-casting for solid oxide fuel cells», J. Mater. Chem., 17 (25), 2627-2635 (2007); b) «Synthesis and performance of $(La_{0.75}Sr_{0.25})_{1-x}(Cr_{0.5}Mn_{0.5})O_3$ cathode powders of solid oxide fuel cells by gel-casting technique», J. Electrochem. Soc., 154, B577-B582 (2007).
10. J.C. Ruiz-Morales, D. Marrero-López, J. Canales-Vázquez, H. Lincke and P. Núñez, «Lanthanum chromite materials as potential symmetrical electrodes for Solid Oxide Fuel Cells», Bol. Soc. Esp. Ceram. V., 46, 218-223 (2007).
11. J. Sfeir, P.A. Buffat, P. Möckli, N. Xanthopoulos, R. Vasquez, H.J. Mathieu, J. van Herle and K.R. Thampi, «Lanthanum chromite based catalysts for oxidation of methane directly on SOFC anodes», J. Catal., 202, 229-244 (2001).
12. O. A. Marina, N. L. Canfield and J. W. Stevenson, «Thermal, electrical, and electrocatalytical properties of lanthanum-doped strontium titanate », Solid State Ionics, 149, 21-28 (2002).
13. J. Canales-Vázquez, S. W. Tao and J. T. S. Irvine, «Electrical properties in $La_2Sr_4Ti_6O_{19-\delta}$: a potential anode for high temperature fuel cells», Solid State Ionics, 159, 159-165 (2003).
14. R. Mukundan, E. L. Brosha and F. H. Garzon, «Sulfur tolerant anodes for SOFCs », Electrochem. Solid-State Lett., 7 [1], A4-A7 (2004).
15. M.D. Gross, J.M. Vohs and R.J. Gorte, «A strategy for achieving high performance with SOFC ceramic anodes», Electrochem. Solid-State Lett, 10, B65-B69 (2007).
16. D.P. Fagg, V.V. Kharton, J.R. Frade and A.A. L. Ferreira, «Stability and mixed ionic-electronic conductivity of (Sr, La) (Ti, Fe) $O_{3-\delta}$ perovskites», Solid State Ionics, 156, 45-57 (2003).
17. D. P. Fagg, J. C. Waerenborgh, V. V. Kharton and J. R. Frade, «Redox behaviour and transport properties of $La_{0.5-x}Sr_{0.5-x}Fe_{0.4}Ti_{0.6}O_{3-\delta}$ ($0<x<0.1$) validated by Mössbauer spectroscopy», Solid State Ionics, 146, 87-93 (2002).
18. a) C. Y. Park and A. J. Jacobson, «Thermal and chemical expansion properties of $La_{0.2}Sr_{0.8}Fe_{0.55}Ti_{0.45}O_{3-x}$», Solid State Ionics, 176 (35-36), 2671-2676 (2005).; b) C.Y. Park and A.J. Jacobson, «Electrical conductivity and oxygen non-stoichiometry of $La_{0.2}Sr_{0.8}Fe_{0.55}Ti_{0.45}O_{3-x}$», J. Electrochem. Soc., 152, J65-J73 (2005).
19. J. Canales-Vázquez, J.C. Ruiz-Morales, D. Marrero-López, J. Peña-Martínez, P. Núñez and P. Gómez-Romero, «Fe-Substituted (La,Sr)TiO_3 as Potential Electrodes For Symmetrical Fuel Cells (SFCs)», J. Power Sources, 171-172, 551-556 (2007).
20. J. Rodríguez-Carvajal, «Recent advances in magnetic structure determination by neutron powder diffraction», Phys. Rev. B, 192, 55-69 (1993).
21. a) J. Canales-Vázquez, M. J. Smith, J. T. S. Irvine and W. Zhou, «Studies on the reorganisation of extended defects with increasing n in the perovskite-based $La_4Sr_{n-4}Ti_nO_{3n+2}$ series», Adv. Funct. Mater., 15, 1000-1008 (2005); b) J. Canales-Vázquez, J.C. Ruiz-Morales, B. Ballesteros, D. Marrero-López and J.T.S. Irvine, «Performance of cubic-(La,Sr)$TiO_{3+\delta}$ as SOFC anodes», Bol. Soc. Esp. Ceram. V., 46, 304-310 (2007).
22. M.A. Alario-Franco, J.M. González-Calbet, M. Vallet.Regí and J.C. Grenier, «Brownmillerite-Type Microdomains in the Calcium Lanthanum Ferrites: $Ca_xLa_{1-x}FeO_{3-y}$», J. Solid State Chem., 49, 219-231 (1983) and references therein.
23. E. H. Mountstevens, J. P. Attfield, S. A. T. Redfern, «Cation-size control of structural phase transitions in tin perovskites», J. Phys.: Condens. Matter., 15, 8315-8326 (2003).
24.a) E. H. Mountstevens, S. A. T. Redfern, J. P. Attfield, «Order-disorder octahedral tilting transitions in $SrSnO_3$ perovskite», Phys. Rev. B, 71, 220102R (2005); b) C. J. Howard, K. S. Knight, B. J. Kennedy, E. H. Kisi, «The structural phase transitions in strontium zirconate revisited», J. Phys.: Condens. Matter., 12, L677-L683 (2000).
25 R. H. Mitchell, Perovskites: Modern and Ancient. Almaz Press: Ontario, Canada, 2002, Chapter 2.
26 a) W. Massa, Crystal structure determination 2nd Edition, Springer-Verlag, Berlin Heidelberg, 2004, Chapter 10; b) A. J. Dos santos-García, G. Heymman, H. Huppertz, M. Á. Alario-Franco, «Turning points in solid-state, materials and surface chemistry». Royal Society of Chemistry Edited Text. RSC Publishing, 2007, Chapter 9
27 a) M. Walden, X. Lai, K. Luo, Q. Guo, D.W. Goodman, «Onset of catalytic activity of gold clusters on titania with the appearance of non-metallic properties», Science, 281, 1647 (1998); b) J. T. Miller, A. J. Kropf, Y. Zha, J. R. Regalbuto, L. Delannoy, C. Louis, E. Bus and J. A. van Bokhoven, «Effect of gold particle size on Au-Au bond length and reactivity toward oxygen in supported catalysts», J. Catal., 240, 222-234 (2006).

Recibido: 30.10.07
Aceptado: 31.03.08